electronics

MDPI

Article

A Novel Feeding Technique for a Quadrifilar Helix Antenna

Alessandro Di-Carlofelice [†], **Emidio Di-Giampaolo** [*,†] **and Piero Tognolatti** [†]

Department of Industrial and Information Engineering and Economics, University of L'Aquila, I-67100 L'Aquila, Italy; alessandro.dicarlofelice@univaq.it (A.D.-C.); piero.tognolatti@univaq.it (P.T.)

* Correspondence: emidio.digiampaolo@univaq.it; Tel.: +39-0862434412

† These authors contributed equally to this work.

Abstract

This paper proposes a novel method for feeding a half-turn quadrifilar helix antenna (QHA) operating in backfire mode. A self-phasing and self-supporting antenna is obtained using a specific method demonstrated numerically. Four straight parallel wires, by which a couple of short-circuited stubs are realized and connected in series with helix loops, constitute both the mast of the QHA and the feeding network. A prototype operating at 1 GHz is designed, realized, and measured. The results show a good axial ratio (measured cross-polar gain is about 25 dB below the co-polar one at the boresight) and good impedance matching over an adequately large frequency band.

Keywords: quadrifilar helix antenna; circular polarization; backfire mode; moment method; feed network

1. Introduction

The ability to receive or transmit a wide beam of circularly polarized radiation while minimizing unwanted radiation is imperative to maintaining good communication in many applications, e.g., satellite-based services and 5G. The axial-mode helical antenna provides a high-performance and robust antenna platform both in space and on the ground. The quadrifilar helix antenna (QHA) was invented by C.C. Kilgus in 1968, who has published several papers establishing the theoretical basis for its operation [1]. The proper choice of helical parameters can provide different radiation patterns with extremely small sizes and weights [2,3]. A QHA consists of two identical bifilar helices that are orthogonal and excited in time-phase quadrature; these characteristics allow for the radiation of a circularly polarized electromagnetic field. Proper quadrature currents can be obtained by using several methods. A well-accepted way to feed a QHA requires quadrature hybrids and baluns to be located apart from the antenna [4,5]. A self-phasing device [6] employs a parallel connection of the two loop inputs and requires loops of different sizes in order to have quadrature currents. Alternative techniques include the use of an integrated coupler [7,8] and Wilkinson power divider [9,10]. In [11], a quadrifilar helical antenna has all the radiating arms connected at the top of the antenna, resulting in wide impedance bandwidth and axial ratio bandwidth with a compact size. In [12], a helix antenna was fed with a traditional circular transmission line with a load resistor. Recently, the evolution of QHA architecture has been heavily oriented towards printed technology (i.e., PQHA) in which the antenna branches are printed on flexible supports and then glued onto dielectric cylinders [13–15]. Typically, these antennas use a feeder network made with a PCB and positioned at the base of the cylinder to impart the necessary phase difference between the antenna branches [16,17]. These networks are often also used to allow for a broadening

Check for updates

Academic Editors: Ikmo Park and Chaouki Hannachi

Received: 7 November 2025
Revised: 2 December 2025
Accepted: 16 December 2025
Published: 21 December 2025

Copyright: © 2025 by the authors. Licensee MDPI, Basel, Switzerland. This article is an open access article distributed under the terms and conditions of the Creative Commons Attribution (CC BY) license.

of the matching band and to excite multimode [18]. A particular case is proposed in [19] in which a four-phase antenna feeder was used to provide the appropriate amplitudes and phases. Another area is the research of low-profile QHA architectures for automotive applications, as shown in [20], where miniaturization is performed both by pursuing a low thickness and by reducing the base area. However, the aforementioned feed networks inevitably increase the dimensions, complexity, and cost of QHA. The on-field adjustment of loop sizes, however, is sometimes difficult or impossible. The present contribution proposes a novel technique that can be used to feed a QHA without any external network and that enables the capability to trim the antenna in order to obtain the best axial ratio and return loss. A numerical analysis for demonstrating the effectiveness of the method is reported. The antenna uses a quad mast (QM-QHA), allows for self-phasing, and does not require helices with different sizes.

2. Rationale of Antenna Design

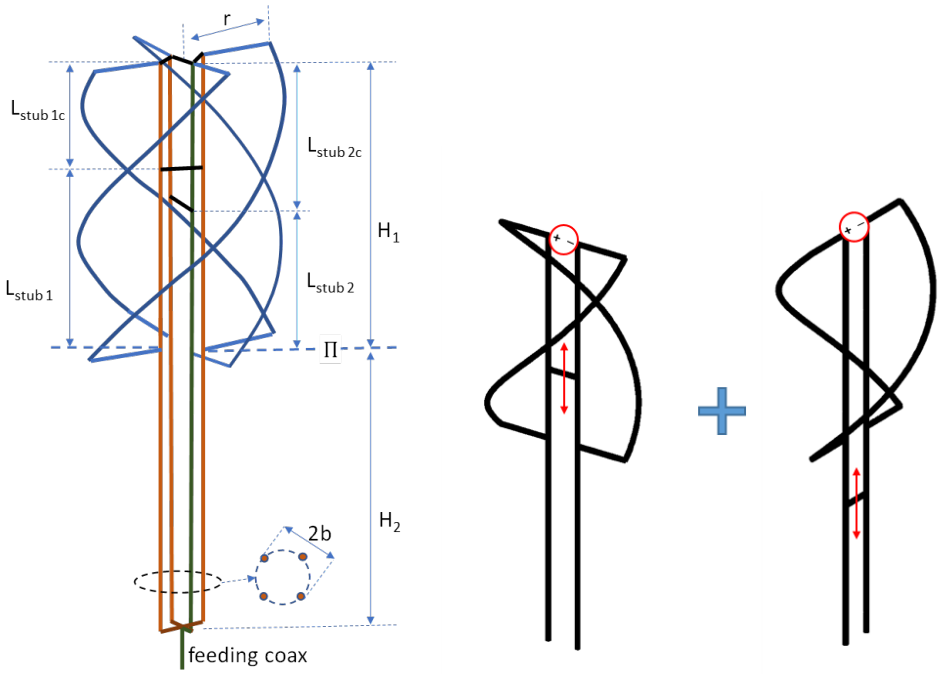
The proposed QHA consists of two couples of half-turn helices (i.e., two bifilars) that are top-fed in phase quadrature at the feeding gap located at the center of the top radial. As shown in [2], the best performance in terms of polarization purity, input impedance, and beam shape is obtained when the current distribution in the helical loops is symmetrical i.e., the exciting signals are in phase quadrature with equal amplitude, which is the condition for obtaining circular polarization.

Using $Y_{1(2)}$ to denote the input admittances of the two bifilars and Y_{in} the input admittance of the whole antenna, conditions for the best performance can be written in terms of the equations shown in the following system:

$$\begin{cases} Y_1 - Y_2 = 0, \\ \angle Y_1 - \angle Y_2 = 90^\circ, \\ \mathrm{Re}\left(\dfrac{1}{Y_{\mathrm{in}}}\right) = 50. \end{cases} \tag{1}$$

where we assumed a desired antenna input resistance of 50 Ω and the two bifilars uncoupled because of geometrical construction. Evidently, in the case of bifilars with equal length, the first equation of System (1) is intrinsically satisfied, while the second one cannot be fulfilled without additional circuit elements. The introduction of short-circuited stubs in series with each bifilar is an easy theoretical solution to simultaneously satisfy the equations of (1), but it requires a novel feeding system to avoid the derangement of the structure of the antenna. The proposed novel feeding system consists of four straight parallel wires by which four short-circuited stubs are realized. Two of them are connected in series with the two bifilars and can be considered as an additional degree of freedom for System (1), while the other two, which are in parallel to the input port, are not independent. As shown in Figure 1, stubs lay on mutually orthogonal planes: stub 1 is in series with one bifilar (e.g., bifilar 1), while stub 2 is in series with the orthogonal one. Stub 1c and stub 2c are a byproduct of the proposed structure; they are given by the complementary part of the four wires with respect to the input ports of bifilars. For this reason, their length cannot be chosen arbitrarily while they have an effect on the input impedance of the antenna. The equivalent circuit of the QM-QHA antenna is shown in Figure 2 where each bifilar is represented as a two-port network. The equivalent circuit neglects the portion of the mast that is below the helix arms since it is chosen with length $H_2 = \lambda/4$.

https://doi.org/10.3390/electronics15010028



(**a**) Complete antenna structure. (**b**) Enlarged antenna structure.

Figure 1. Half-turn quadrifilar helix antenna with proposed feeding network: (**a**) whole structure with relevant parameters; (**b**) separated bifilars with corresponding sliding short circuit of stubs and generators.

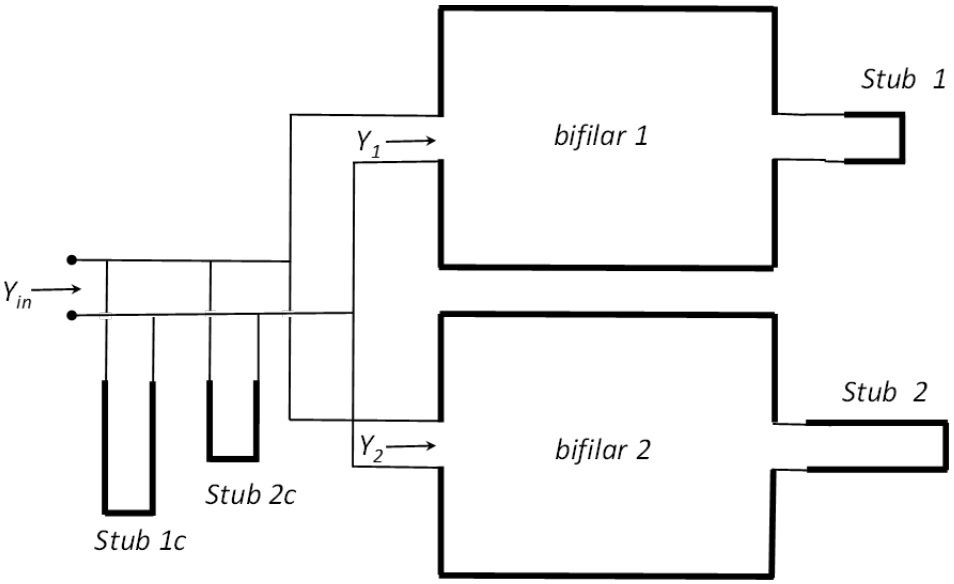


Figure 2. Equivalent circuits of QHA shown in Figure 1.

The use of stubs provides a couple of degrees of freedom that permits the tuning of the input admittance of each bifilar. The sliding of the short circuits of the stubs along the parallel wires permits us to find a position for which the input admittances at the feeding gaps have the same magnitude and are in phase quadrature at the desired frequency. The same four wires constitute a quad mast that serves as the mechanical support of the helical elements and allow a coaxial line to reach the feeding gap implementing an "infinite balun" [21]. Due to the upward radiation, a ground plane can be added without any major effect. The appropriate choice of which of the two branches of a bifilar is powered by the inner conductor of the coaxial cable and which by the external conductor permits us to determine the upward direction of radiation. The choice of LHCP or RHCP polarization

instead is imposed by choosing the right-handed or left-handed twisting direction to the helix. To find the lengths of stubs, different optimization objectives can be imposed; we chose to impose the radiation null condition in the backward direction of the radiation pattern since it is a peculiarity of that antenna, as reported in [1–3]. The fulfillment of that condition in fact always corresponds to the best axial ratio in the direction of the maximum radiation [2] so that it is an indirect resolution of the first two equations of System (1). More solutions (i.e., different stub lengths) satisfy the backward null condition, but not all of them permit us to satisfy the third equation of System (1). A numerical demonstration of this behavior was achieved with an exhaustive search by varying the length of both stubs (1 and 2). The proposed feeding structure, nevertheless, is sensitive to coupling with bifilars, so the dimensioning of the stubs to fulfill System (1) has to be determined by taking into account the currents flowing over bifilars. For this reason, a full-wave model of QM-QHA was developed with Altair Feko (MoM solver) [22] where the values of the stub lengths were considered unknown, while the other relevant parameters were kept fixed at chosen values to make the hand-made realization of the antenna easy. The resonant frequency is assigned at 1 GHz, while the characteristic impedance of the stub lines is chosen as 297 Ω, equivalent to that of a parallel two-wire transmission line with conductors with a radius of $\lambda/300$ slid and a spacing ($2b$ in Figure 1) of 0.04λ (λ is the wavelength). The numerical analysis was repeated for all possible combinations of the lengths of the two stubs in the interval $[-\lambda/4, \lambda/4]$ with step $\lambda/100$. The negative sign is used to indicate stubs that extend from the reference plane Π (Figure 1) toward the base of the mast. At each step, the front-to-back ratio (F/B), the axial ratio (AR), and the real (R) and imaginary (X) parts of the input impedance are calculated, and the achieved results are shown in Figure 3 as a contour map. For visibility reasons, only the part of the map that allows us to find a solution is shown in Figure 3. There are four regions of the map where F/B is greater than 20 dB, and these are labeled with letters 'a', 'b', 'c', and 'd' in Figure 3. They correspond to four possible structures satisfying the objective of obtaining a high value of F/B. The possible structures have an $AR > 0.9$ in 'a', $0.85 < AR < 0.9$ in 'b', $AR \cong 0.85$ in 'c', and $AR \cong 0.9$ in 'd'. The real part of the input impedance R is a little bit smaller than 50 Ω in 'a', centered at 50 Ω in 'b', near 100 Ω in 'c', and about 75 Ω in 'd'. The imaginary part X is positive in all solutions and ranges between 20 Ω in 'c' and 'd' and 40 Ω in 'b', and in 'a', it is about 30 Ω. Since structures 'c' and 'd' have an R that is not compliant with our specifications, our choice is limited to 'a' and 'b'. We choose 'a' since it has an AR greater than that of 'b', while its X is smaller. The structure 'a' can be considered a solution of System (1). In any case, to make $X \cong 0$, it is necessary to put a series capacitance at the input port of the antenna. The values of stub lengths for the found solution 'a' are reported in Table 1 together with the other relevant parameters.

Table 1. Parameters of antenna structure.

$\mathbf{H_1}[\lambda]$	$\mathbf{H_2}[\lambda]$	$\mathbf{L_{stub1}}[\lambda]$	$\mathbf{L_{stub2}}[\lambda]$	$\mathbf{r}[\lambda]$	$\mathbf{b}[\lambda]$	**⌀ Wire** $[\lambda]$	**C** $[pF]$
0.25	0.25	0.085	0.035	0.085	0.02	1/150	5.0

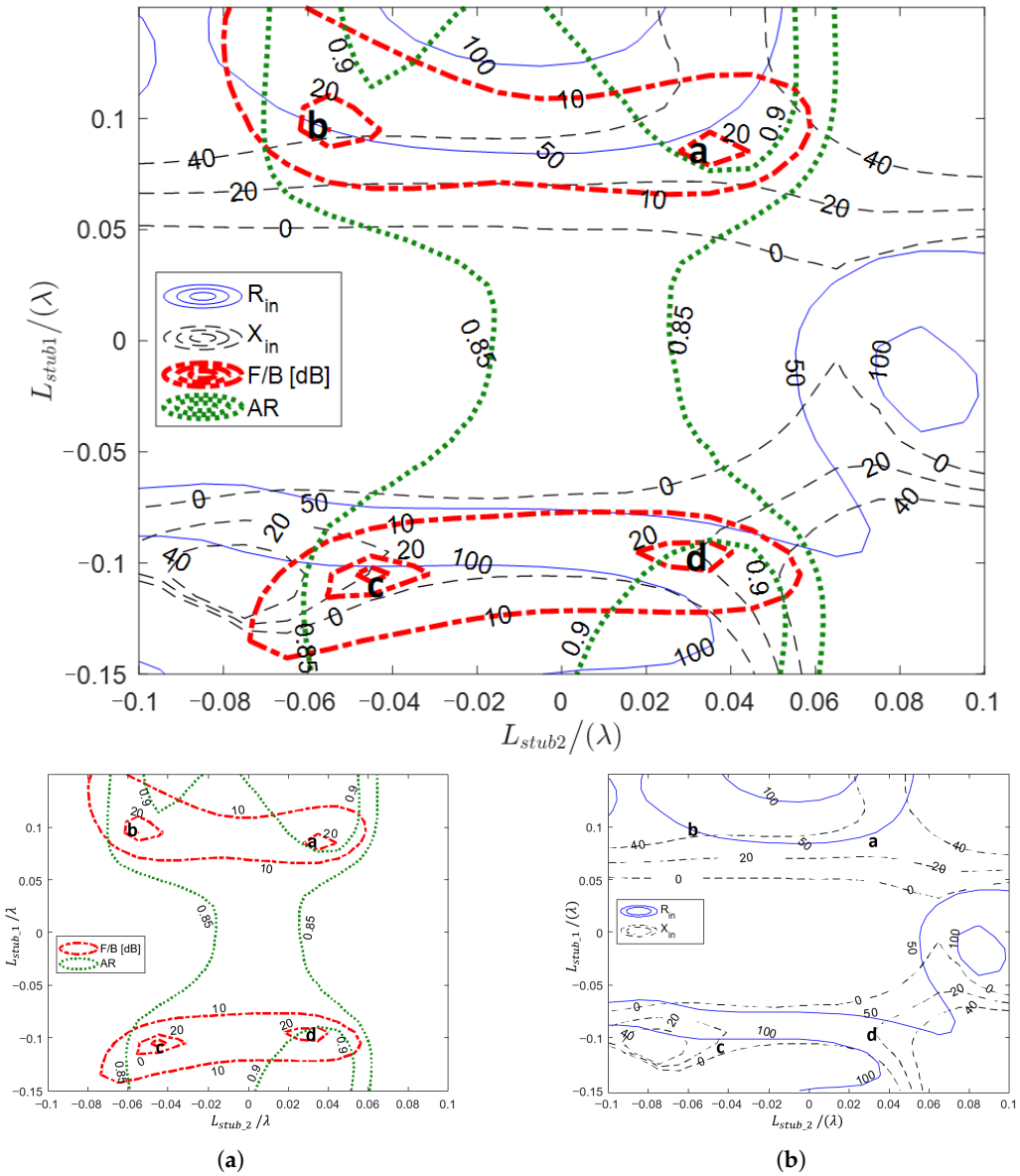


Figure 3. Superimposed contour maps of numerical results for different couples of stub lengths: F/B ratio (bold, dashed red line); AR (dotted green line); real and imaginary parts of antenna impedance (continuous blue and dashed black lines, respectively). (**a**,**b**) are separated maps.

3. Numerical and Experimental Results

An LHCP QM-QHA @1GHz was designed and realized. The body of the antenna together with the mast was made with a UT-085 coax cable; only the external conductor was used, aside from the feeding line.Tunable stubs were realized with metallic strips tightened to the vertical lines of the mast by means of rubber bands. Figure 4 shows the color map of the numerically calculated magnitude of the currents over the antenna structure at two different time instants with time-phase quadrature. This result confirms the effectiveness of the method given that the currents reversed above the two bifilars at the two instants of time. The prototype antenna pattern was measured using Starlab multi-probe systems at MVG Italia [23] (Figure 5). The simulated and measured results were compared. As shown in Figure 6, the prototype antenna has a very good matching impedance at the design frequency; the change in the reflection coefficient with frequency agrees with that obtained numerically; and in both the model and prototype, a series capacitance of 5 pF at

the input port was included. The bandwidth at −10 dB is about 64 MHz. The front-to-back ratio is reported in Figure 7 where the fulfillment of the imposed optimization condition for the numerical model is apparent, and the discrepancy in the measured results can be attributed to inaccuracies in the hand-manufacturing of the prototype. In fact, an in-depth numerical analysis demonstrated complete agreement between numerical and measured F/B if the length of bifilars in the model was 0.005λ shorter. The axial ratio at the boresight is reported in Figure 8; it is around 0.9 for frequencies lower than 1.02 GHz, while it is decreasing at higher frequencies. Inside the impedance matching bandwidth, $AR < 1$ dB. The agreement between the model and the prototype is not perfect, but the discrepancy is as small as a fraction of dB. Figure 9 shows directivity vs. frequency. A fair agreement between the model and the prototype was achieved, and the maximum directivity for the model is 5.4 dB @1GHz, while the prototype has 5.23 dB @1.01GHz. The efficiency is about 91% accounting for the losses of the coaxial cable and connector. Co-polar and cross-polar patterns for all directions were quickly measured, and the two principal cuts for $\phi = 0°$ and $\phi = 90°$ are shown in Figures 10 and 11, respectively. Evidently, measurement and simulation agree well over a large extension of the main lobe for the co-polar component, while the discrepancy for the cross-polar component concerns values lower than −10 dB. The half power beam width is about 119.5° for $\phi = 0°$ and 116.5° for $\phi = 90°$, revealing the substantial circular symmetry of the radiation pattern. Table 2 shows a comparison of the main characteristics of the proposed antenna with those of the QHA reported in the literature. It is observed that the proposed antenna has a gain and an axial ratio (AR) comparable to or better than that of the others, while for bandwidth, a direct comparison is not always applicable as many antennas are made using printed technology with a matching network and designed for wide or multi-band bandwidths. A direct comparison is possible between those belonging to the self-phasing antenna family, where the results obtained are well aligned with those shown in the literature.

Table 2. A comparison with the literature.

Ref.	Technology	Op. Freq. (GHz)	BW (MHz)	Gain (dB)	AR (dB)
[6] *	printed	1.575	12	2.7	0.8
[7]	printed	1.176/1.575	30/72	4.2/2.1	2
[13]	printed	1.227/1.575	100/100	3.6/4.2	0.9
[14]	printed	1.6	300	2.2	N.A.
[15]	printed	1.227/1.575	20/10	5.1/4.1	<3
This work *	wire	1.0	64	5	<1

* self-phasing, N.A. Not Available.

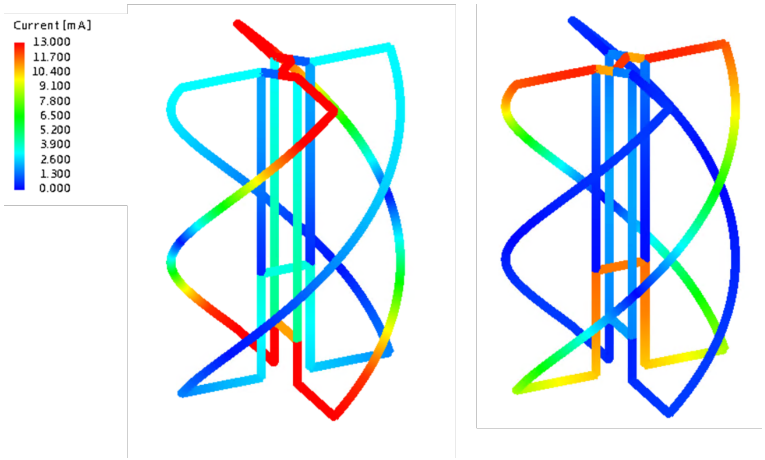


Figure 4. Color map of magnitude of currents over antenna structure (numerical results). Two pictures correspond to time instant with time-phase quadrature.

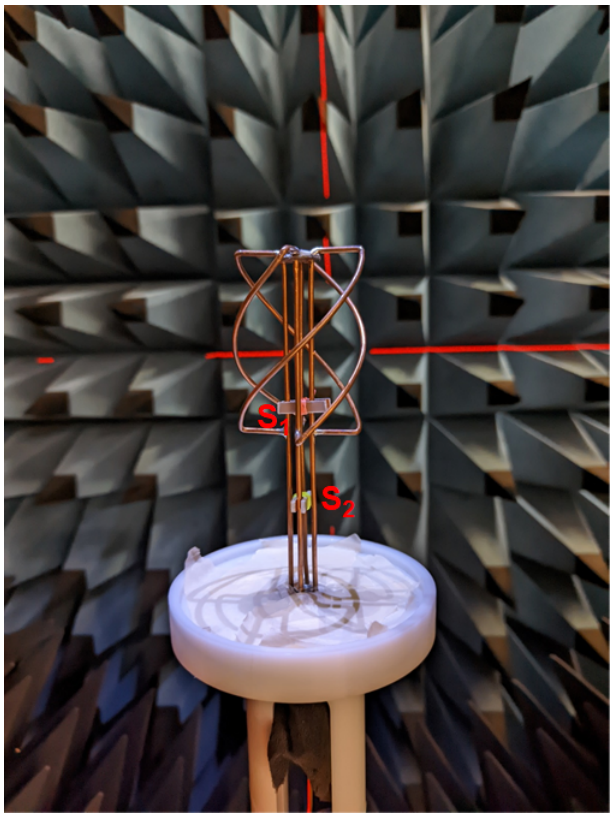


Figure 5. The realized prototype antenna inside the StarLab measurement equipment. The sliding short circuits of stubs (S1, S2) are realized with two couples of small copper strips tightened to the vertical lines of the mast by means of rubber bands. The feeding coaxial cable runs inside one of the four vertical lines, implementing the infinite balun.

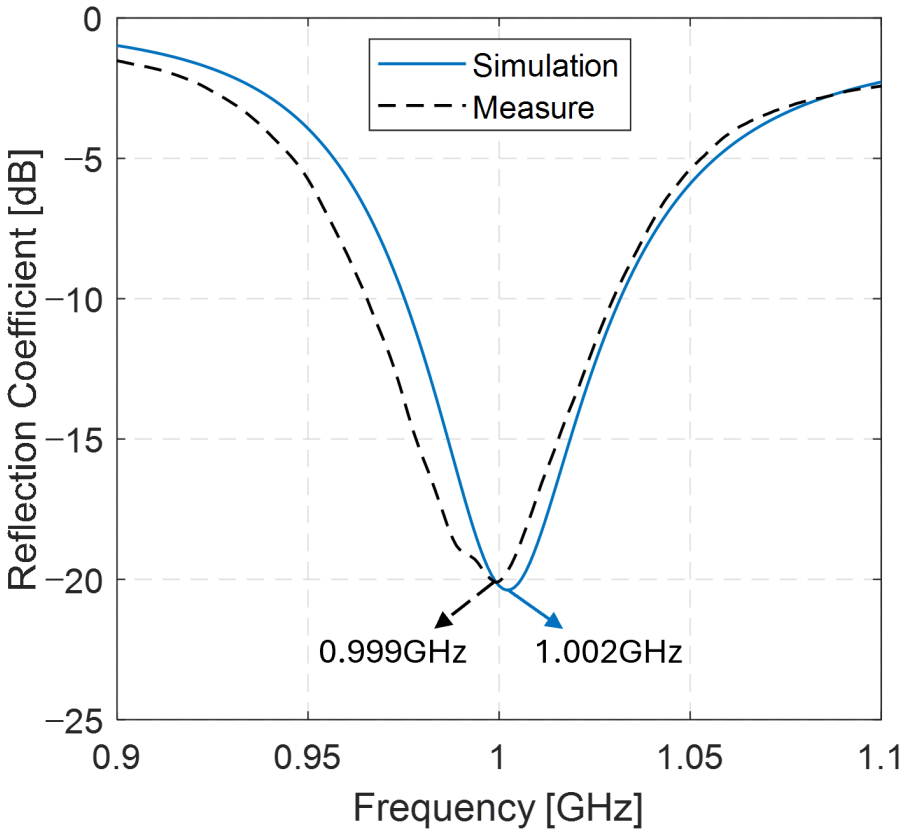


Figure 6. Reflection coefficient: numerical (continuous line); measured (dashed line).

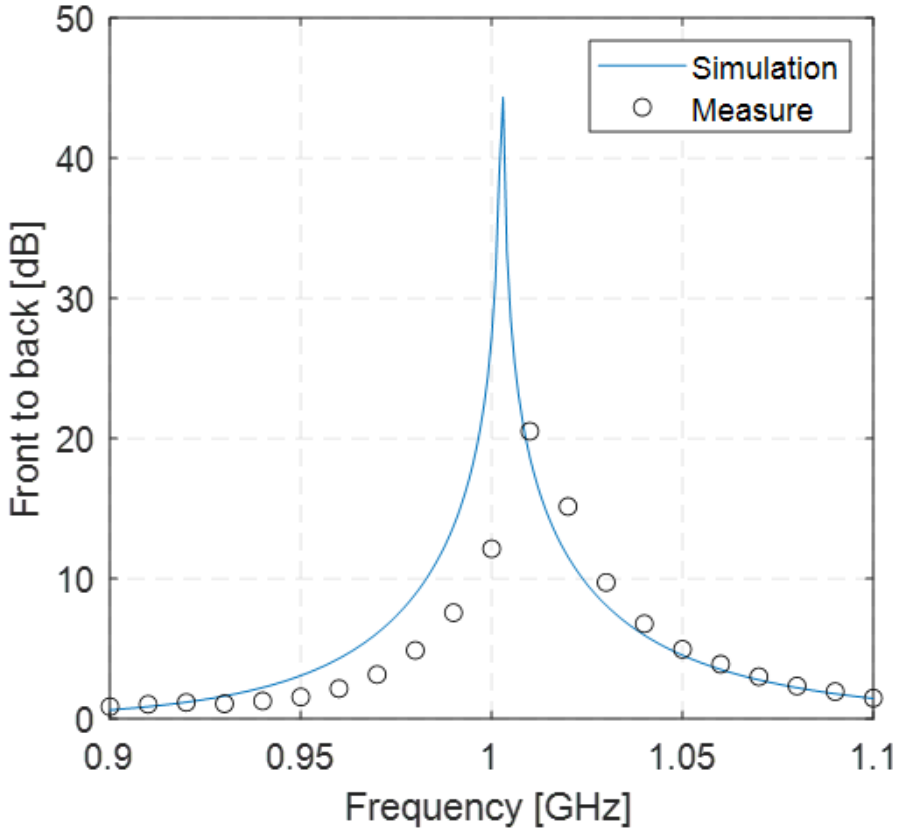


Figure 7. Front- to-back ratio: numerical (continuous line); measured (circles).

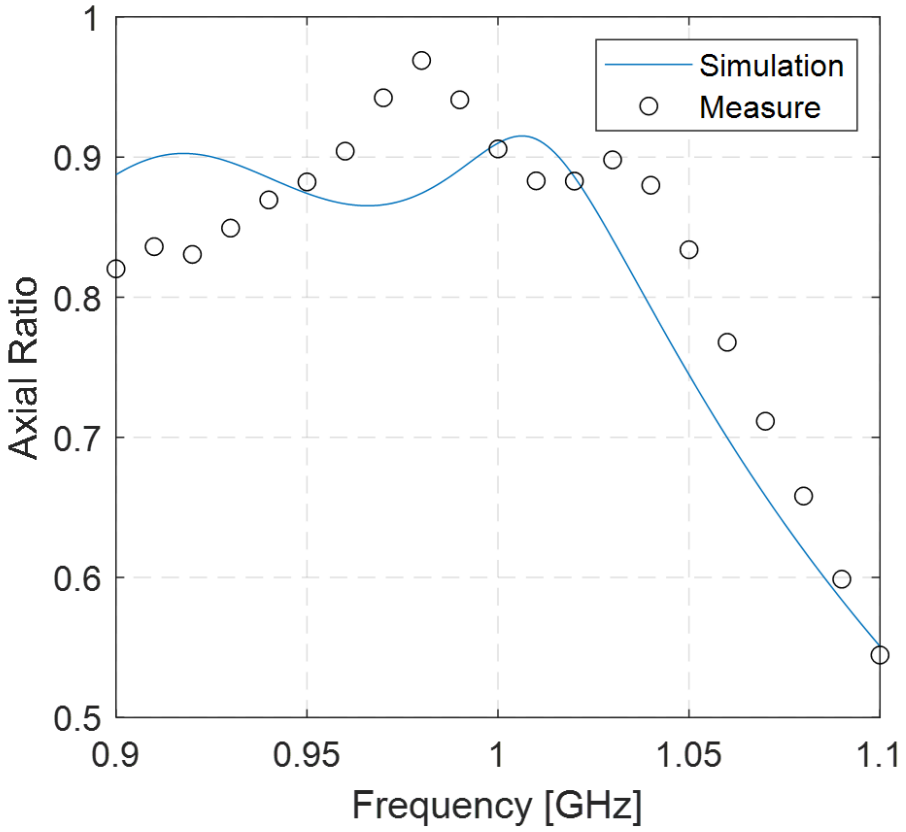


Figure 8. Axial ratio: numerical (continuous line); measured (circles).

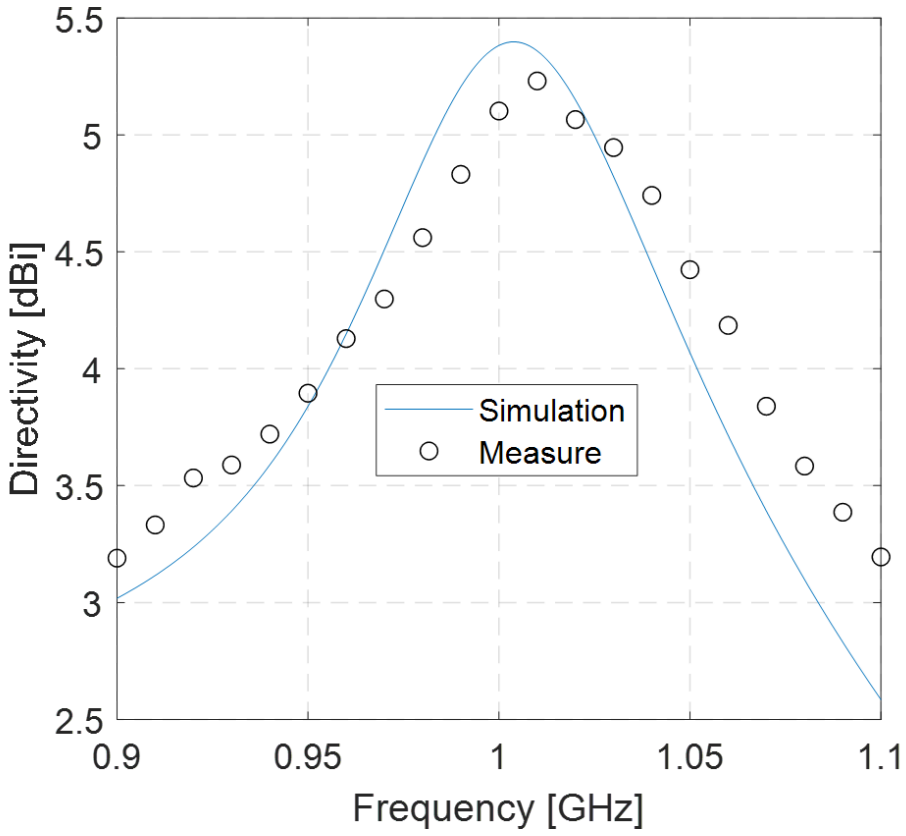


Figure 9. Directivity vs. frequency: numerical (continuous line); measured (circles).

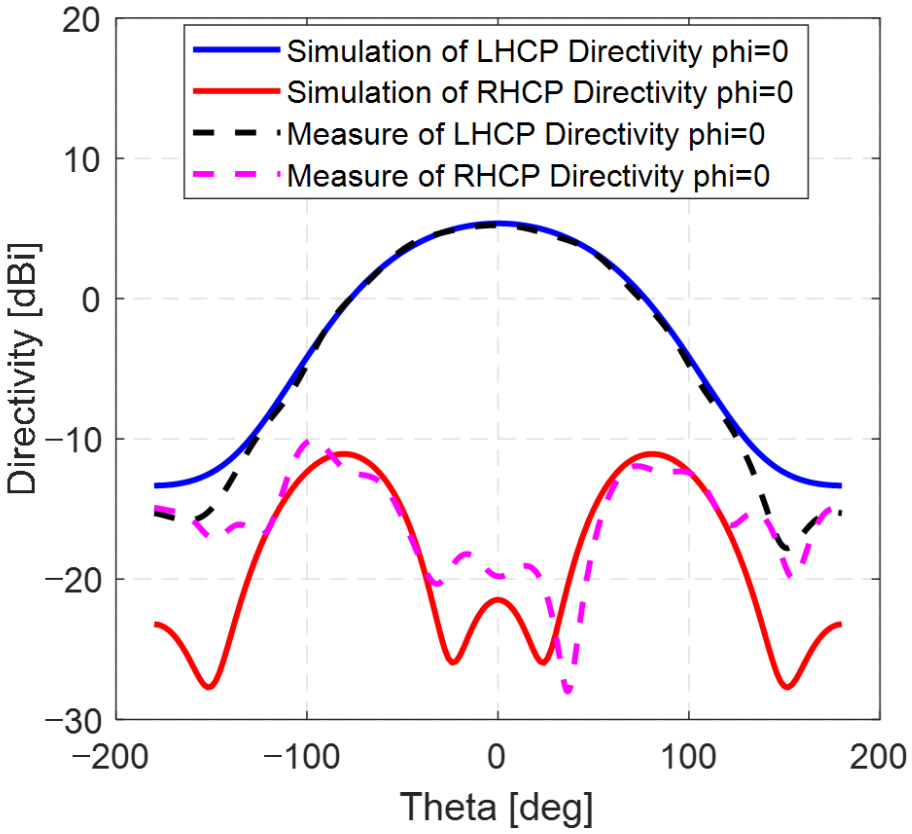


Figure 10. Radiation pattern for $\phi = 0°$: numerical (continuous line); measured (dashed line). Co-polar in blue color; cross-polar in red color.

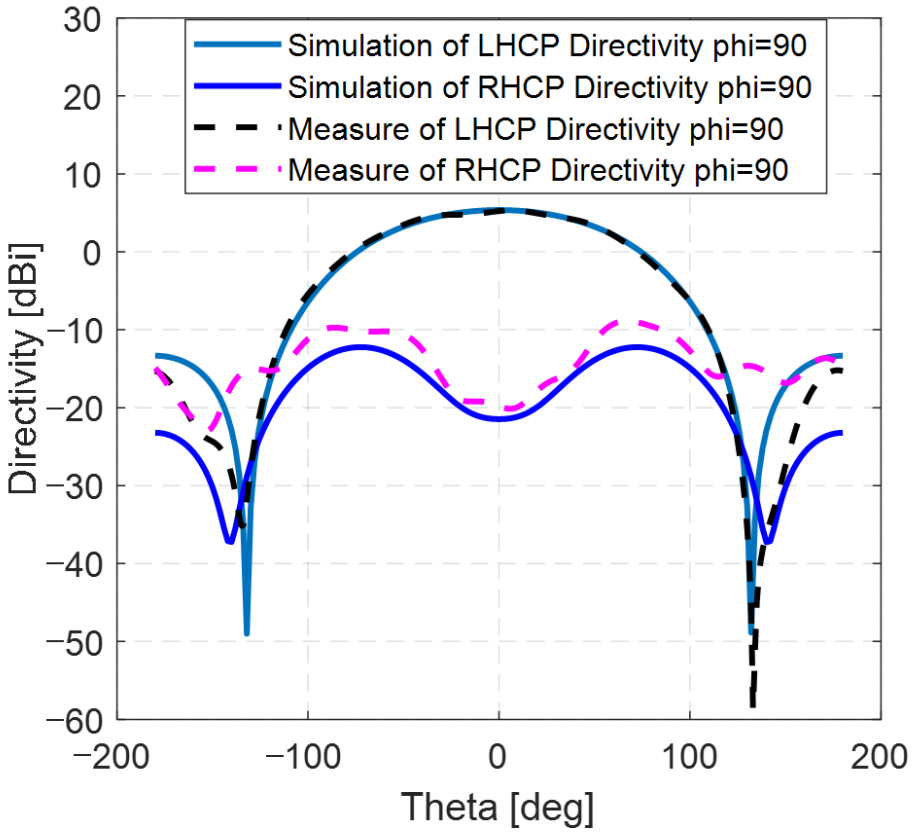


Figure 11. Radiation pattern for $\phi = 90°$: numerical (continuous line); measured (dashed line). Co-polar in blue color; cross-polar in red color.

4. Conclusions

A self-phasing quadrifilar helix antenna based on a quad mast (QM-QHA) structure that permits the sliding of tuning stubs and does not require helices with different sizes was reported. The design method was described and demonstrated. Antenna performances were shown and discussed, comparing the numerical and measurement results. The obtained performance is in agreement with that of the theoretical model and is comparable to the ones of other feeding methods. In particular, our design allows us to achieve a maximum directivity of 5.2 dB with 0.91 efficiency, a bandwidth of 64 MHz, a front-to-back ratio of about 20 dB, and an axial ratio less than 0.9 dB.

Author Contributions: Conceptualization , A.D.-C., E.D.-G. and P.T.; Methodology, A.D.-C., E.D.-G. and P.T.; Validation, A.D.-C., E.D.-G. and P.T.; Formal analysis, A.D.-C., E.D.-G. and P.T.; Investigation, A.D.-C., E.D.-G. and P.T.; Writing—original draft, A.D.-C., E.D.-G. and P.T.; Writing—review & editing, A.D.-C., E.D.-G. and P.T. All authors have read and agreed to the published version of the manuscript.

Funding: This research received no external funding.

Data Availability Statement: Data are contained within the article.

Acknowledgments: The authors wish to thank MVG Italia for carrying out the measurements with its facilities and to Sergio Cicerone for his help in manufacturing the antenna.

Conflicts of Interest: The authors declare no conflict of interest.

References

1. Kilgus, C. Multielement, Fractional Turn Helices. *IEEE Trans. Antennas Propag.* **1968**, *16*, 499–500. [CrossRef]
2. Kilgus, C. Resonant quadrafilar helix. *IEEE Trans. Antennas Propag.* **1969**, *17*, 349–351. [CrossRef]

3. Kilgus, C. Resonant quadrafilar helix design. *Microw. J.* **1970**, *16*, 349–351.
4. Bricker, R.; Rickert, H. An S-band resonant quadrifilar antenna for satellite communication. In Proceedings of the 1974 Antennas and Propagation Society International Symposium, Atlanta, GA, USA, 10–12 June 1974; Volume 12, pp. 78–82. [CrossRef]
5. Sharaiha, A.; Terret, C.; Blot, J. Printed quadrifilar resonant helix antenna with integrated feeding network. *Electron. Lett.* **1997**, *33*, 256–257. [CrossRef]
6. Wang, Y.S.; Chung, S.J. A Miniature Quadrifilar Helix Antenna for Global Positioning Satellite Reception. *IEEE Trans. Antennas Propag.* **2009**, *57*, 3746–3751. [CrossRef]
7. Rabemanantsoa, J.; Sharaiha, A. Size Reduced Multi-Band Printed Quadrifilar Helical Antenna. *IEEE Trans. Antennas Propag.* **2011**, *59*, 3138–3143. [CrossRef]
8. Byun, G.; Choo, H.; Kim, S. Design of a Dual-Band Quadrifilar Helix Antenna Using Stepped-Width Arms. *IEEE Trans. Antennas Propag.* **2015**, *63*, 1858–1862. [CrossRef]
9. Zhang, Z.Y.; Yang, L.; Zuo, S.L.; Rehman, M.U.; Fu, G.; Zhou, C. Printed quadrifilar helix antenna with enhanced bandwidth. *IET Microw. Antennas Propag.* **2017**, *11*, 732–736. [CrossRef]
10. Taherkhani, M.; Tayebpour, J.; Radiom, S.; Aliakbarian, H. Circularly polarised wideband quadrifilar helix antenna with ultra-wide beamwidth isoflux pattern for a S-band satellite ground station. *IET Microw. Antennas Propag.* **2019**, *13*, 1699–1704. [CrossRef]
11. Yi, X.; Huitema, L.; Wong, H. Polarization and Pattern Reconfigurable Cuboid Quadrifilar Helical Antenna. *IEEE Trans. Antennas Propag.* **2018**, *66*, 2707–2715. [CrossRef]
12. Guo, J.; Yang, Y.; Huang, Y.; Sun, B. Slot multi-arm helix antenna with simple and efficient feeding network. *Electron. Lett.* **2015**, *51*, 1224–1226. [CrossRef]
13. Pu, Y.; Wang, H.; Zhao, Y.; Yuan, Y.; Xi, X.; Member, I. Miniaturized wideband quadrifilar helix antenna for satellite navigation application. *Microw. Opt. Technol. Lett.* **2021**, *63*, 252–263. [CrossRef]
14. Khajepour, S.; Ghaffarian, M.S.; Moradi, G. Design of novel multiband folded printed quadrifilar helical antenna for GPS/WLAN applications. *Electron. Lett.* **2017**, *53*, 58–60. [CrossRef]
15. Han, Y.; Wang, H.; Wang, Z.; Yao, Y.; Feng, Y.; Hu, K.; Gao, Y.; Fan, Z.; Yuan, S. Dual-Band Spiral Printed Quadrifilar Helical Antenna Miniaturized by Surface and Inner Dielectric Loading. *IEEE Access* **2019**, *7*, 30244–30251. [CrossRef]
16. Liu, H.; Shi, M.; Fang, S.; Wang, Z. Design of Low-Profile Dual-Band Printed Quadrifilar Helix Antenna With Wide Beamwidth for UAV GPS Applications. *IEEE Access* **2020**, *8*, 157541–157548. [CrossRef]
17. Zhang, W.; Zhang, Q.; Li, S.; Zhao, H.; Yin, X. A Bandwidth-Enhanced Quadrifilar Helix Antenna Using Gaps on Arms for Satellite Communication. In Proceedings of the 2022 IEEE 10th Asia-Pacific Conference on Antennas and Propagation (APCAP), Xiamen, China, 4–7 November 2022; pp. 1–2. [CrossRef]
18. Musthafa, A.M.; Khalily, M.; Araghi, A.; Yurduseven, O.; Tafazolli, R. Compact Multimode Quadrifilar Helical Antenna for GNSS-R Applications. *IEEE Antennas Wirel. Propag. Lett.* **2022**, *21*, 755–759. [CrossRef]
19. Mo, K.; Jiang, X.; Peng, L.; Fang, R. Dual-Sleeves Printed Quadrifilar Helix Antenna With Quad-Band and Ultrawide Beamwidth for Satellite Communication Mobile Terminals. *IEEE Trans. Antennas Propag.* **2025**, *73*, 2395–2404. [CrossRef]
20. Pang, Z.Y.; Tam, K.W.; Zhou, X.; Zhang, Z.; Chen, Q.; Liu, J.; Sio, H.P.; Chen, R.S.; Huang, G.L. A Low-Profile Circularly Polarized Spring-Shaped Quadrifilar Helical Antenna for Vehicle Satellite Navigation Systems. *IEEE Trans. Veh. Technol.* **2025**, *74*, 14267–14276. [CrossRef]
21. Johnson, R.A.; Jasik, H. *Antenna Engineering Handbook*, 2nd ed.; McGraw-Hill Inc.: New York, NY, USA, 1984.
22. Altair. Available online: https://altair.com/feko (accessed on 24 October 2025).
23. Microwave Vision Group. Available online: https://www.mvg-world.com/en (accessed on 24 October 2025).

Disclaimer/Publisher's Note: The statements, opinions and data contained in all publications are solely those of the individual author(s) and contributor(s) and not of MDPI and/or the editor(s). MDPI and/or the editor(s) disclaim responsibility for any injury to people or property resulting from any ideas, methods, instructions or products referred to in the content.